Available online at www.sciencedirect.com
ScienceDirect
C. R. Physique 9 (2008) 642–656
COMPTES RENDUS PHYSIQUE
http://france.elsevier.com/direct/COMREN/

Synchrotron x-rays and condensed matter/Rayonnement X synchrotron et matière condensée

X-ray detected optical activity

Andrei Rogalev *, José Goulon, Fabrice Wilhelm

European Synchrotron Radiation Facility (ESRF), B.P.-220, 38043 Grenoble cedex, France

Available online 16 May 2008

Abstract

Optical Activity (OA) was only measured quite recently in the X-ray range using electric dipole–electric quadrupole interference terms that mix multipoles of opposite parity but are only present in systems with broken inversion symmetry. *Natural* OA refers to effects that are *even* with respect to time-reversal symmetry, whereas *non-reciprocal* OA is concerned with time-reversal odd contributions. Various types of X-ray dichroism related to either natural or non-reciprocal OA have been detected and are reviewed in the present paper. ***To cite this article: A. Rogalev et al., C. R. Physique 9 (2008).***

Résumé

Activité Optique mesurée par rayons X. L'Activité Optique n'a été mise en évidence que très récemment dans le domaine spectral des rayons X où les termes d'interférence dipole électrique–quadrupole électrique couplent des multipoles de transition de parité différente dans des systèmes non-centrosymétriques. L'Activité Optique *naturelle* fait réference à des termes qui sont pairs par rapport à l'opérateur de renversement du temps tandis que les termes d'Activité Optique *non-réciproque* sont impairs par rapport à ce même opérateur. Dans cet article, nous passons en revue différents types de dichroïsme des rayons X qui sont liés tant à l'Activité Optique naturelle qu'aux effets non-réciproques. ***Pour citer cet article : A. Rogalev et al., C. R. Physique 9 (2008).***

Keywords: Natural Optical Activity; Non-reciprocal dichroism; Polarization dependent X-ray spectroscopy

Mots-clés : Activité Optique naturelle ; Dichroïsme non-réciproque ; Spectroscopie des rayons X polarisés

1. Introduction

Natural Optical Activity was discovered by Arago and Biot [1,2] who observed in 1811 the rotation of the plane of polarization of visible light in quartz crystals. In 1845, after numerous unsuccessful attempts, Faraday [3] established that the plane of polarization could also be rotated when a light beam propagated through a sample inserted in a strong magnetic field; this effect was called Magneto-Optical Activity. Even though both experiments result in a rotation of the polarization plane of light, the underlying physics is fundamentally different.

Magneto-optical effects arise as a consequence of *energy dispersion*: the external magnetic field or any exchange field will cause a relative shift of the density of states involved into optical transitions induced by right- and left-

* Corresponding author.
E-mail address: rogalev@esrf.fr (A. Rogalev).

1631-0705/$ – see front matter
doi:10.1016/j.crhy.2008.04.003

circularly polarized light. The important point is that the observation of magneto-optical activity does not require the sample to satisfy any specific symmetry condition because the effect involves pure electric dipole ($E1.E1$) transitions.

Natural OA, in contrast, is a manifestation of *spatial dispersion* [4], i.e. the fact that the transition probabilities also depend on the space variable **r** as well as on the light wavevector **k**. Natural OA refers to the first order terms (linear in k) and require the transition probabilities to mix multipoles of opposite parity, e.g., electric dipole–magnetic dipole ($E1.M1$) or electric dipole–electric quadrupole ($E1.E2$). The Curie symmetry principle states that this is only possible in systems with broken inversion symmetry. Strictly speaking, only OA effects that are *even* with respect to time reversal symmetry, such as optical rotation (OR) or circular dichroism (CD), are referred to as *natural* optical activity or *reciprocal* OA. On the other hand, time-reversal odd OA phenomena do exist as well and are commonly called *non-reciprocal*. The latter effects should not be confused with the magneto-optical effects that are also time reversal-odd: *non-reciprocal* OA can only be observed in parity-odd magneto-electric media.

Since its discovery, optical activity of visible light has developed as one of the most powerful spectroscopic tools in physics, chemistry and biology and has fascinated many successive generations of scientists. The existence of optical activity in the X-ray range has remained a fully open question for nearly one century until X-ray Natural Circular Dichroism (XNCD) was unambiguously detected at the ESRF in quite a few non-centrosymmetric crystals [5–8]. What made such experiments feasible was the recent availability of intense beams of circularly polarized X-rays at third-generation synchrotron radiation sources. Let us underline, however, that the origin of OA effects is fairly different in the visible and in the X-ray spectral regions. The reason for that is that the $E1.M1$ interference terms, which dominate OA in the visible range, become vanishingly small in X-ray spectroscopy because magnetic dipole transitions ($M1$) from deep core levels are forbidden, at least in non-relativistic theories. In contrast, $E1.E2$ interference terms which will be shown to play a major role in the X-ray range [9,10], are often negligible at optical wavelengths. Various types of X-ray dichroisms related to either natural or non-reciprocal OA have now been measured at the ESRF and are reviewed in the present paper.

In Section 2 we shall make use of the gyration tensor formalism to introduce a variety of X-ray dichroisms related to OA: this formalism is most helpful to clearly identify various effects that can be expected in a non-centrosymmetric crystal. In Section 3 we will discuss how to optimize OA measurements in the hard X-ray range. In Section 4, we have selected some typical experimental results to illustrate the detection of either natural and non-reciprocal OA effects. Finally, in the last section we discuss briefly the edge-selective sum rules [11] which make it possible to identify the effective operators responsible for X-ray detected optical activity.

2. X-ray detected optical activity in the gyration tensor formalism

X-ray detected OA can be most easily described using a complex *gyration* tensor which takes into account spatial dispersion effects, i.e. the breakdown of the usual electric dipole approximation in radiation-matter interactions. A quick way to introduce this tensor is to use the theory of refringent scattering which was elaborated by Buckingham and his colleagues [12,13] for OA in the visible. We have shown elsewhere how to extend this theory into the X-ray regime [14]. Let us recall that an important implication of this approach is that all modes propagating inside the crystal should be parallel to the wave vector of the incident beam: this requirement is quite acceptable in the X-ray range where the real part of the refractive index $n = 1 - \delta$ is very close to unity since $\delta \leqslant 10^{-5}$ so that critical angles for X-ray reflection $\Theta_c = \sqrt{2\delta}$ are in the range of few mrads.

For a transverse polarized wave with a wavevector **k** the forward scattered amplitude is a complex tensor $\mathbf{a}^\star$ that can be expanded in series as:

$$a^*_{ij} = \alpha^*_{ij} + \zeta^*_{ijl}k_l + \left(\frac{1}{4}Q^*_{illj} + \frac{1}{6}\eta^*_{illj}\right)k_l^2 + \cdots \tag{1}$$

The first term refers to the rank-2 electric dipole complex polarizability tensor ($\alpha^* \propto E1.E1$). It is fully symmetric and describes the linear birefringence and dichroism effects. In the presence of an external magnetic field or spontaneous magnetic order, this tensor has an antisymmetric part that is related to the Faraday effect and the magnetic circular dichroism. Further terms in the symmetrical part that are quadratic in the magnetization describe the Cotton–Mouton effect and the magnetic linear dichroism.

The last terms in Eq. (1) involves two complex rank-4 tensors: the first one is the pure electric quadrupole polarizability tensor ($Q^* \propto E2.E2$) whereas the second one is the electric dipole–electric octupole interference term

Table 1
Irreducible parts of the gyration tensor in SO(3)

Odd parity crystal classes	Point groups	Pseudo-scalar	Polar vector	Pseudo-deviator
		Enantio-morphism	Voigt/Fedorov	XNCD
$\bar{4}3$ m $\bar{6}$ m $\bar{6}$	T_d D_{3h} C_{3h}	NO	NO	NO
432 23	O T	YES	NO	NO
622 32 422	D_6 D_3 D_4	YES	NO	YES
6 mm 3 m 4 mm	C_{6v} C_{3v} C_{4v}	NO	YES	NO
6 3 4	C_6 C_3 C_4	YES	YES	YES
$\bar{4}2$ m	D_{2d}	NO	NO	YES
$\bar{4}$	S_4	NO	NO	YES
mm2	C_{2v}	NO	YES	YES
222	D_2	YES	NO	YES
2	C_2	YES	YES	YES
m	C_s	NO	YES	YES
1	C_1	YES	YES	YES

($\eta^* \propto E1.E3$). There has been ample experimental evidence produced in these recent years [15] that the electric quadrupole ($E2.E2$) contribution could become quite significant in X-ray Absorption Spectroscopy (XAS). Typically, the electric quadrupole polarizability tensor may give rise to an optical anisotropy in cubic crystals which was observed in the visible [16,17] as well as in the X-ray range [18,19]. It may be worth emphasizing here that the electric dipole–electric octupole interference term mixes multipole moments of the same parity and hence cannot contribute to OA.

We are most concerned in the present paper with the second term in Eq. (1) since it is precisely the complex, rank-3 gyration tensor ($\zeta^* \propto E1.E2$ or $E1.M1$). In the absence of any external magnetic field or any spontaneous magnetic ordering in the system, ζ^* is fully antisymmetric and describes effects related to natural OA, i.e. the reciprocal optical rotation, the natural circular birefringence and circular dichroism. Let us stress again that the elements of the gyration tensor are associated with transition probabilities that mix multipoles of opposite parity, and, thus, can be non-zero only in non-centrosymmetric systems.

The gyration tensor has three irreducible representations with respect to the operations of the rotation group SO_3 [20]:

- A pseudo-scalar part associated only with the $E1.M1$ interference term which is commonly detected at optical wavelengths in enantiomorphous (chiral) systems;
- A polar vector part resulting from both $E1.M1$ and $E1.E2$ interference terms: it is associated with a (very) weak longitudinal component of electrical polarization that may eventually result in pyroelectric ordering;
- A rank-2 pseudo-deviator part to which both $E1.M1$ and $E1.E2$ interference terms contribute.

As far as X-ray spectroscopy is concerned, magnetic dipole transitions ($M1$) are forbidden by well-known selection rules. Nevertheless, as first pointed out by Goulon [9], the interference between the electric dipole and electric quadrupole $E1.E2$ can still contribute to OA in the X-ray range. This point was supported by more recent theories [21–23]. In this context, only the vector part and the pseudo-deviator can contribute to OA in the X-ray range. Since a pseudo-deviator is a traceless object, X-ray detected OA can hardly be measured in a sample without orientational order, e.g., in a powder or a solution. It immediately appears here that *chiral enantiomorphism* and *Optical Activity* are two distinct concepts which should never be confused.

Not all non-centrosymmetric crystals will exhibit OA in the X-ray range: following Jerphagnon and Chemla [20], we have listed in Table 1 which of the 21 classes of non-centrosymmetric crystals should be compatible with the detection of natural OA in the X-ray range. Table 1 makes it clear that only 13 crystal classes will admit a *pseudo-deviator* as rotational invariant in SO(3) and can exhibit X-ray Natural Circular Dichroism (XNCD) as a consequence of a non-vanishing gyration tensor $\zeta^* \propto E1.E2$. On the other hand, it appears also from Table 1 that the so-called Voigt–Fedorov dichroism can be observed only in 10 crystal classes which admit a polar vector as irreducible representation.

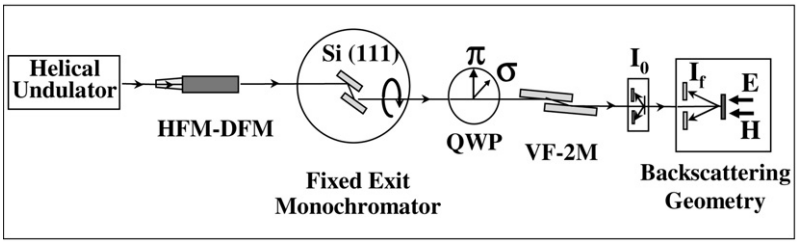

Fig. 1. Conceptual block diagram of the ESRF beamline ID12: HFM-DFM = horizontally focusing & deflecting mirrors; QWP = Quarter wave plate assembly; VF-2M = Vertically focusing double mirror; I_0 = photodiode intensity monitors; I_f = photodiode X-ray fluorescence detectors.

When a crystal is odd not only with respect to space parity but also with respect to the time-reversal operator, the gyration tensor ζ^* may still exhibit a symmetric part: this term is at the origin of a variety of non-reciprocal OA effects, such as non-reciprocal or gyrotropic birefringence, non-reciprocal Linear Dichroism, magneto-chiral birefringence and dichroism. Magnetoelectric (or multiferroic) solids appear as good candidates to detect such effects since, as pointed out by Dzyaloshinskii [24], the temporal and spatial inversion symmetries are broken in these systems which remain invariant with respect to the product of both symmetry operations. There are up to 58 Shubnikov groups that are compatible with the magnetoelectric effect [25]. We have analyzed elsewhere [11] which dichroic effect could be measured for a given magnetoelectric group.

If we limit ourselves to dichroism experiments only, it can be shown that every component of the Stokes polarization vector of the incoming X-ray beam is associated with a well identified dichroism related to OA:

- $S_0 \Rightarrow$ X-ray magnetochiral dichroism (XMχD) [26];
- $S_1 \Rightarrow$ non-reciprocal X-ray magnetic linear dichroism (nr-XMLD) [27];
- $S_2 \Rightarrow$ Jones non-reciprocal cross XMLD (Jones XMLD);[1]
- $S_3 \Rightarrow$ X-ray natural circular dichroism (XNCD) [5] and Voigt–Fedorov dichroism [28].

3. Instrumentation and experimental considerations

X-ray dichroism is classically defined as the difference in the X-ray absorption cross sections for two orthogonal polarization states of the incident beam: e.g. right- and left-handed polarization for circular dichroism, σ and π polarization for linear dichroism measurements, etc. Given the fact that the amplitude of the dichroic signal can be as small as a few parts in 10^4 compared to the total absorption cross section, the beamline should be carefully designed if one wishes to make sure that such tiny dichroism signals can be measured free of artefacts. The experiments reported in this paper were all carried out at the ESRF beamline ID12 which was specifically optimized for XAS applications requiring a full control of the polarization of the X-ray photons over the energy range 2–15 keV. The concept of the beamline is illustrated schematically in Fig. 1. Since the performance of this beamline has already been discussed in full details elsewhere [29,30], let us simply underline briefly here a few selected points which, in practice, are absolutely essential to carry out successful OA experiments.

Either circularly or linearly polarized X-ray photons can be generated by any one of the three helical undulators installed on the ID12 straight section: HELIOS-II [31], APPLE-II and the so-called "ElectroMagnet Permanent magnet Hybrid Undulator" (EMPHU) [32] are three undulators that were optimized to complement each other. The latter is most appropriate for experiments at low photon energies ($E \ll 4$ keV) but it also makes it possible to flip very rapidly (≈ 160 ms) the circular polarization of the emitted photons from left to right; on the other hand, the Helios-II (HU-52) or Apple-II (HU-38) undulators offer – at a much longer timescale – a perfect control of the photon polarization with much higher photon fluxes, especially at high energy.

The monochromator is the most critical component in any XAS spectrometer because the quality of the experimental spectra can easily be spoiled by a poor energy resolution, the transmission of unwanted harmonics or instabilities of the exit beam during energy scans, etc. The ESRF beamline ID12 is equipped with a UHV compatible, fixed-exit,

[1] To the best of our knowledge this dichroism has not yet been detected.

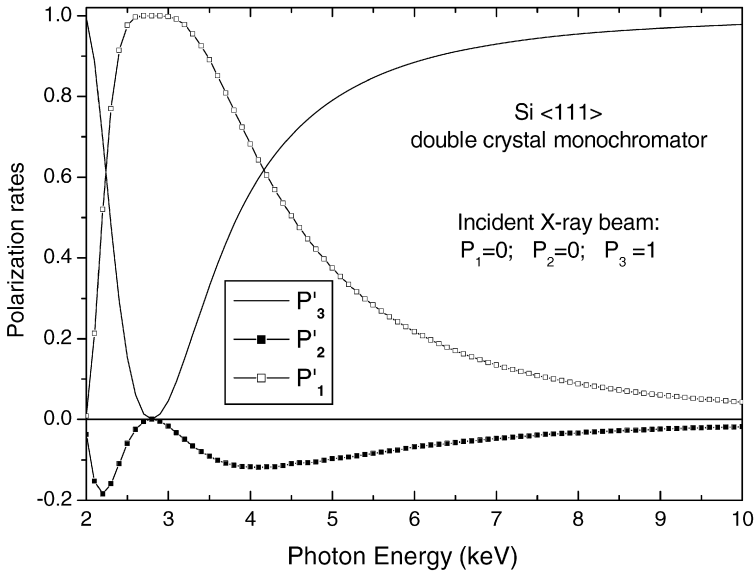

Fig. 2. Calculated polarization rates of the X-ray beam monochromatized by Si ⟨111⟩ double-crystal monochromator. The incident X-ray beam is completely circularly polarized.

double-crystal monochromator manufactured by KoHzu Seiki Co. The exceptional quality of the mechanics, in particular the high precision of the translation stages, allows one to obtain a fixed exit beam (within ±5 μm) over the whole angular range (6°–80°). The monochromator is usually equipped with a pair of Si ⟨111⟩ crystals. Note that the temperature of each individual crystal is kept near −140 °C (±0.2°) by a cryogenic cooling system developed in-house and which proved to be completely vibration free. The stability of the maximum of the rocking curve was found to be better than 0.1 arcsec over periods of several hours. For two consecutive energy scans, we obtained an excellent reproducibility of typically 1 meV or better.

As far as X-ray circular dichroism experiments are concerned, one should keep in mind that the initial degree of polarization of the undulator beam cannot be preserved downstream from the double crystal monochromator, except for completely σ or π polarized beams. We performed a number of numerical simulations regarding the transfer of polarization by a Si ⟨111⟩ double-crystal monochromator. The calculated polarization rates of the of the monochromatic X-ray beam (the Stokes–Poincaré components P'_1, P'_2, P'_3) as a function of the photon energies in the range 2–10 keV are shown in Fig. 2.

The calculations were performed assuming that the incoming undulator beam is fully circularly polarized ($P_3 = 1$). One will notice that for photon energies around 2.8 keV the values of P'_3 are extremely low, this makes X-ray circular dichroism measurements difficult in the corresponding energy range. Indeed, this condition corresponds to the Brewster angle ($\Theta_B = 45°$) at which the monochromator acts as a perfect linear polarizer ($P'_1 = 1$). As a consequence of the fairly different reflectivity of the σ and π-components, the linearly polarized component with the polarization vector at ±45° is also generated by the monochromator even though the incident beam is completely circularly polarized. This P'_2 component could be rather intense (nearly 20% at 2.2 keV) and is proportional to the P_3 component of the incident X-ray beam. This has very important practical consequences: whenever the helicity of the undulator beam is reverted, not only the circular polarization of the monochromatic X-ray beam is altered but there is also a significant change of P'_2, whereas P'_1 remains unaffected. This can have a dramatic effect on circular dichroism measurements (including XNCD as well as XMCD) in the case of *biaxial* crystals because a weak circular dichroism signal can be easily masked by a much stronger linear dichroism signal [33,34]. Some similar difficulty is to be expected for measurements on uniaxial crystals whenever the optical axis of the sample is not strictly parallel to the direction of propagation of the X-rays.

In order to fully characterize the polarization state of the monochromatic beam, we have inserted downstream from the monochromator a UHV compatible Quarter Wave Plate (QWP) chamber equipped with a diamond single

crystal [35]. For X-ray linear dichroism (XLD) experiments, one may also exploit the QWP to convert the circularly polarized incident X-ray beam into a linearly polarized beam with a freely adjustable azimuthal angle [29]. Moreover, it is straightforward to switch rapidly from one linear polarization to the orthogonal one. In this way, it becomes feasible to flip the polarization vector several times for each data point of a spectral scan with the advantage that the experiment becomes inherently much less sensitive to low-frequency instabilities of the source so that small linear dichroism signals can be measured much more accurately.

Nearly all optical activity experiments carried out at the ESRF beamline ID12 concerned thick single crystals which were much too absorbing for measurements in the transmission mode. All spectra were then systematically recorded in the total X-ray fluorescence yield mode using photodiodes as detectors. The backscattering geometry of these detectors was found most attractive since it makes it possible: (i) to set the optical axis of the crystal perfectly collinear with the wavevector **k** of the incident X-ray photons; and (ii) to rotate the crystal around the direction of the wavevector **k**. The latter option is crucial for OA experiments on biaxial systems. Last but not least, in the case of magnetoelectric solids, the sample can be inserted inside a bore of a superconducting electromagnet so that a magnetic field **H** and an electric field **E** both parallel to the wavevector **k** can be applied simultaneously for magnetoelectric annealing, as schematically shown on Fig. 1.

4. Natural Optical Activity with X-rays

4.1. X-ray Natural Circular Dichroism

X-ray Natural Circular Dichroism (XNCD) refers to the difference in the X-ray absorption cross-sections measured respectively with left- and right-circularly polarized X-ray photons in the absence of any magnetic field. The first experiment establishing unambiguously the existence of XNCD was carried out at the ESRF in 1997 using a uniaxial *laevo*-rotatory crystal of α-$LiIO_3$ which belongs to the enantiomorphous crystal class 6 [5]. Surprisingly, a rather large XNCD signal (amounting to ca. 6% with respect to the edge jump) was observed at the iodine L_1 absorption edge. At the L_2 and L_3 edges, XNCD spectra were recorded that had strictly the same sign and very similar spectral shapes: this point is quite remarkable since XMCD spectra most often exhibit opposite signs at the L_2 and L_3 edges. This can be easily understood if one keeps in mind that spin–orbit and exchange splitting are the driving forces in XMCD, while this is not the case for XNCD, at least if the signal is to be assigned to $E1.E2$ interference terms as anticipated. Moreover, this result also leaves very little hope of detecting any significant contribution of the pseudo-scalar $E1.M1$ interference term that should strongly depend as well on spin–orbit interactions. Our interpretation was also fully supported by a comparison of the experimental spectra with ab initio simulations based on a theory developed in the framework of Multiple Scattering Waves (MSW) analyses [21,23].

Systems that exhibit a well-resolved pre-edge feature (assigned to $1s \rightarrow 3d$ quadrupolar transitions) on the low energy side of the K-edge spectra of transition metals [15] were obviously good candidates for further XNCD studies. As an illustration, we have reproduced in Fig. 3 the cobalt K-edge XAS and XNCD spectra recorded with two enantiomeric single crystals of a chiral *propeller-like* organometallic complex $2[Co(en)_3Cl_3]\cdot NaCl\cdot 6H_2O$, in which the ligand field has the enantiomorphous D_3 point group symmetry [8]. Note that the organometallic complex $[Co(en)_3]^{3+}$ ion has long served as a paradigm in the structural and theoretical chemistry of chiral transition metal compounds.

As one can judge from Fig. 3, the XNCD signal is not marginally small in the pre-edge region and, as expected, it has the opposite sign for the two enantiomers. Such a large magnitude of the XNCD signal confirmed our expectation that the $E1.E2$ transition probabilities were quite significant at the K-edge of transition metals. The corresponding Kuhn asymmetry factor $g = (\sigma^L - \sigma^R)/(\sigma^L + \sigma^R)$ was found to be of the order of 12.5% at the Co K-edge: this is comparable with the g factor (22%) of $d - d$ excitations in the visible which are indeed dominated by $E1.M1$ transition probabilities. Interestingly, we have also compared in Fig. 3 the XNCD spectra recorded either with a single crystal or using a pellet of a powdered sample of the same enantiomer [11]. In the case of the powdered sample, there is a very weak XNCD signal (nearly 30 times smaller) which has *the opposite sign* with respect to the XNCD measured with the single crystal. To explain the puzzling presence of such a weak XNCD with the powdered sample, one may envisage two different options:

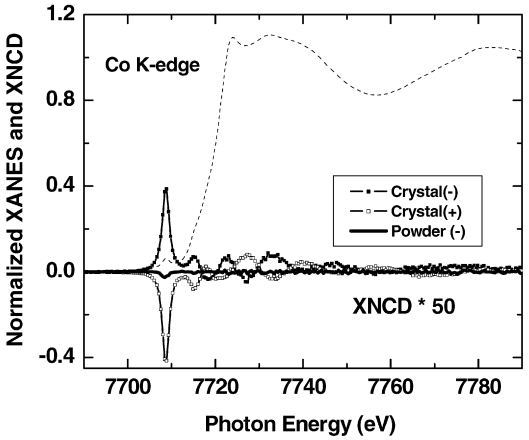

Fig. 3. Co K-edge XNCD of the resolved enantiomers of the chiral complex: $2[Co(en)_3Cl_3]\cdot NaCl\cdot 6H_2O$. XNCD spectrum recorded with a single crystal of the (+) enantiomer and XNCD spectra ot the (–) enantiomer as single crystal or as a powdered pellet. A polarisation averaged XANES spectrum was added for the sake of comparison. Note the very weak signal of the powdered sample.

(i) the effect could possibly be due to a residual orientational order in the pellet, since the angular dependence of the XNCD signal from a uniaxial crystal has a form $\sigma_L - \sigma_R \propto (3\cos^2\theta - 1)$ where θ denotes the angle between the optic axis of the crystal and the X-ray wavevector [21];

(ii) it could be assigned to a very weak $E1.M1$ scalar interference term. Whereas monoelectronic $M1$ transitions from a $1s$ core level to $3d$ states are strictly forbidden in any non-relativistic formalism, they become weakly allowed in relativistic theories [36]. Moreover, $E1.M1$ transitions could become allowed for a multielectron process such as a *two* electron excitation involving (for instance) the transition of one core electron to a fully symmetric $A1$ state and a simultaneous $d \rightarrow d$ transition.

Whatever the true interpretation may be, this experiment sets the highest limit of the $E1.M1$ contributions to natural optical activity in the hard X-ray range. When no single crystal is available, one may still play some trick to recover a weak XNCD signal due to the $E1.E2$ interference term: the idea is to artificially break the orientational isotropy of space, e.g. by investigating chiral molecules dissolved in a liquid crystal aligned in a high magnetic field. Such a successful experiment was reported elsewhere [11].

Let us stress that the detection of XNCD signals is not restricted to the near-edge region of the absorption spectrum: we have produced clear evidence that XNCD signatures can extend over a much wider energy range. Oscillations of the XNCD signal were observe which we may refer to as *Chiral-EXAFS* (χ-EXAFS) because these oscillations could be seen as the analog of Magnetic-EXAFS for XNCD. It was shown that χ-EXAFS oscillations originate only from selected, symmetry allowed, *multiple-scattering* paths because any single scattering path is intrinsically achiral since it transforms into itself by a mirror plane. Taking full advantage of the availability of the EMPHU source which allowed us to flip rapidly the helicity of the X-rays, we were able to detect such EXAFS-like oscillations at the L_I-edge of Te using an uniaxial crystal of α-TeO_2 [34]. We found it possible to identify which were the multiple-scattering paths that had the largest contribution to the XNCD signal. Simulations carried out using the MSW formalism have shown that the chiral paths involving the nearest oxygen neighbours represent the dominant contribution whereas chiral paths involving the heavy Te scatterers give a very broad spectrum and suffer from a large Debye–Waller damping. The final conclusion was that, in the X-ray range, most of the natural dichroism signal could be accounted for by a chiral arrangement of the low-Z oxygen atoms surrounding the Te absorber.

Despite the initial expectation that XNCD could only be a small effect, we proved that it can readily be measured in oriented non-centrosymmetric systems. Moreover, its sign can be correlated with the absolute configuration of the relevant chiral structure via the $E1.E2$ interference terms: XNCD does not provide us simply with an element specific probe of local chirality but it can also afford a unique quantitative information regarding the amount of mixing of orbitals of different parity at the absorbing site. Such a piece of information should be of direct interest to explain or predict the non-linear optical properties of crystals.

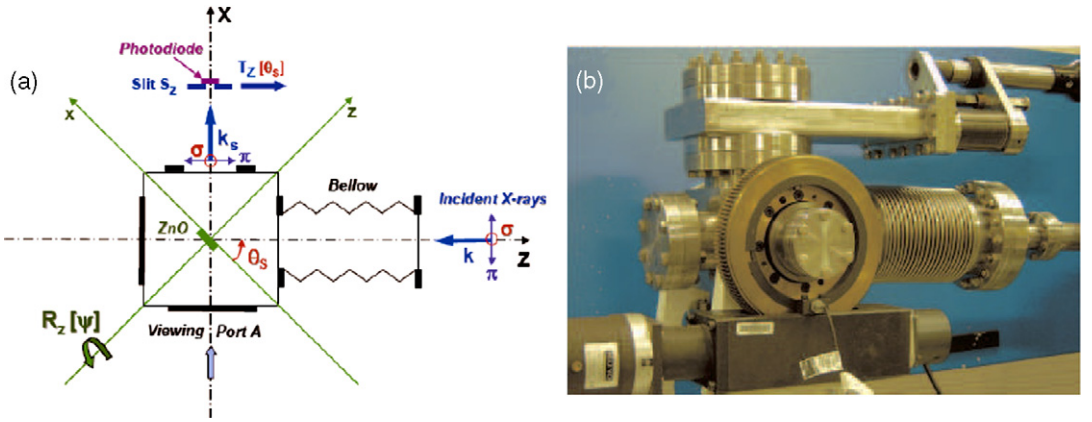

Fig. 4. XNCD experimental set-up: (a) schematic view of the diffractometer. Notice that the crystal **c** axis is perpendicular to the scattering plane for $\psi = \pm\pi/2$; (b) overall view of the diffractometer with its rotating chamber and playless wormscrew.

4.2. Detection of the vector part of Optical Activity using X-rays

In this section, we shall focus on systems in which the gyration tensor has an irreducible part that transforms as a polar vector in SO(3). As following from Table 1, there are 3 classes of non-centrosymmetric crystals (4 mm, 3 m, 6 mm) which look most attractive because the corresponding gyration tensors have only an irreducible part that transforms as a vector. In other terms, crystals which belong to those classes do not exhibit any optical rotation nor any natural circular dichroism: this is why such crystals are often (improperly) quoted as *optically inactive*.

In 1905 Voigt [37] was the first to suggest that such crystals should nevertheless exhibit OA. An experiment to detect such a peculiar OA was proposed by Fedorov [38] in 1959: his idea was that, in crystals of suitable symmetry, an oblique incident linearly polarized light could be reflected as an elliptically polarized light. Shortly later, Fedorov et al. [39] envisaged which specific geometry of the experiment could maximize the amplitude of this effect at optical wavelengths. Unfortunately, it took still quite a long time until the reality of vector type OA was established: the first successful experiment with visible light was reported only in 1978 by Ivchenko et al. [40] who investigated the OA of an hexagonal CdS crystal in the exciton resonance region.

More recently, the theory of reflectivity in non-centrosymmetric uniaxial crystals was carefully revisited by Graham and Raab [41]. The important outcome of their contribution was to show that the most appropriate tests to detect the vector part of OA are measurements of Circular Intensity Differences (CID) in reflectivity when the crystal **c** axis is perpendicular to the reflection plane and when the angle of incidence is close to 45°. Unfortunately, specular reflectivity of X-rays cannot be used for such measurements because the off-diagonal terms responsible for optical activity just vanish at glancing angles. However, we suggested recently that the vector part of OA could still be measured in the X-ray resonant diffraction regime using circularly polarized X-rays at Bragg angles near 45° for which the crystal will act as a linear polarimeter.

The first experiment of this type [28] has been performed again at the ESRF ID12 beamline simply adapting a UHV reflectometer initially designed for other purposes and featuring an excellent mechanical reliability and a high reproducibility [42]. In the configuration illustrated with Fig. 4, a UHV compatible six-way port stainless-steel chamber could be rotated about a horizontal axis (Y) perpendicular to the diffraction plane [X, Z] defined with respect to the laboratory frame {X, Y, Z}. Note that {x, y, z} is the reference frame of the sample, not to be confused with the symmetry axes of the crystal. In this experiment, we were concerned with Bragg angles of the order of $\theta_s \simeq 45°$. The detector had then to be located along the $2\theta_s$ direction, i.e. at about 90° from the incident beam or close to the vertical (X) axis. For convenience, the 2θ scan was replaced by a trivial translation (T_Z) of a narrow slit (≈ 0.5 mm) located in front of the detector at about 14 cm of the sample. An azimuthal rotation ($\Delta\psi$) about the sample axis (z) was implemented using a compact, in-vacuum stepper motor attached to the sample holder. For such a challenging experiment, we selected a high-quality zincite crystal that has the desired hexagonal symmetry (würtzite structure). For our experiment, we excited the strong (300) reflection, the Bragg angle of which varies from 43.13° to 42.69°

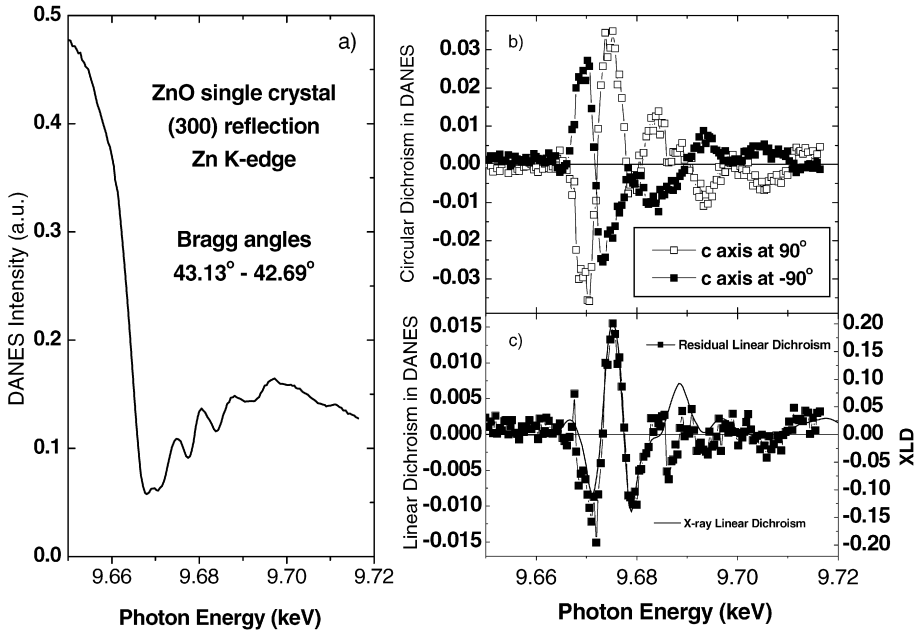

Fig. 5. Circular Difference Intensities (CID) of the Zn K-edge DANES spectra for the ZnO (300) reflection: (a) Polarization averaged DANES spectrum; (b) CID Spectra in the DANES regime for two orientations of the crystal; (c) Comparison of the asymmetry (residual) signal with the XLD spectrum.

over the whole Zn K-edge XANES range (9655–9735 eV). It is noteworthy that the zinc atoms contribute 80% of the structure factor of this reflection. Under such conditions, the angular width of the reflection was typically 5.4 arcsec.

The most typical results of our experiments are reproduced in Fig. 5. The Zn K-edge DANES (Diffraction Anomalous Near Edge Structure) spectrum reproduced in Fig. 5(a) was measured with the crystal **c** axis perpendicular to the scattering plane: what is plotted in Fig. 5(a) is simply the integrated area below the (300) diffraction peak as a function of the incident photon energy. The CID spectra shown in Fig. 5(b) were obtained from the difference between DANES spectra recorded with either left- or right-circularly polarized incident X-ray photons. Graham and Raab were the first to point out that the sign of the CID signal should be reversed if the crystal was rotated by 180° around the normal to the reflection planes, i.e. when the angle between the **c** axis of the crystal and the reflection plane is changed from $+90°$ to $-90°$. This is exactly what we observed, as illustrated in Fig. 5(b). Note that such a 180° rotation should leave unchanged any (unwanted) residual *linear dichroism* provided that the diffraction planes are strictly perpendicular to the rotation axis. Thus, in the absence of any artefact, one would expect the sum of the X-ray CID spectra recorded at $\pm 90°$ to reproduce accurately the X-ray Linear Dichroism (XLD) spectrum generated by the existence of a small P_2' polarization component in the output beam of monochromator (ca. 2% at 9.7 keV). As illustrated with Fig. 5(c), the residual spectrum obtained in this way reproduces well the XLD spectrum measured simultaneously in the total fluorescence yield detection mode.

This experiment clearly establishes the possibility to measure the vector part of X-ray detected OA. Given that ZnO belongs to a very important class of pyroelectric materials, we expect this experiment to open the way to new element and orbital selective studies of ferroelectric crystals of appropriate symmetry.

5. Non-reciprocal X-ray Detected Optical Activity

5.1. Non-reciprocal X-ray Linear Dichroism

Here, we are concerned with a non-reciprocal X-ray Magnetic Linear Dichroism (nr-XMLD), i.e. the difference between the absorption cross-sections measured with orthogonal (σ,π) components of linearly polarized X-rays. Recall that this new effect should be odd with respect to time-reversal symmetry and can be observed only in magnetic crystals with broken inversion symmetry. In order to avoid any confusion, let us stress that such an XMLD signal

related to OA is fundamentally different from the magneto-optical XMLD effect discovered by Van der Laan et al. [43] since the latter is a time-reversal *even* effect.

As first pointed out by Birss and Shrubsall [44] and confirmed later by several authors [45,46], non-reciprocal OA effects should be detected in crystals which are *magnetoelectric*. Magnetoelectric systems belong to the special class of magnetic ordered materials where both time reversal symmetry and parity are not conserved, while the combined symmetry operation is conserved. The corresponding optical effect, i.e. the non-reciprocal magnetic linear dichroism, is notoriously small in the visible region and was difficult to exploit experimentally [47,48].

Even though there are as many as 58 magnetoelectric crystal classes, it does not mean that nr-XMLD can be easily detected with a magnetoelectric crystal. The geometrical and symmetry requirements to detect this effect were discussed in full details elsewhere [11]. Unfortunately, a major difficulty arises from the fact that magnetoelectric crystals are very often antiferromagnetic and, therefore, do exhibit multidomain states. In order to observe the desired non-reciprocal XMLD effect in an antiferromagnet, one has first to grow a single antiferromagnetic domain and one should manage the capability to switch from one type of domain to the other. This is usually achieved using a still mysterious *"magnetoelectric annealing"* procedure which consists in heating up first the crystal in the paramagnetic phase: after some delay time, an electric and a magnetic field are simultaneously applied before one starts to cool the crystal slowly down across the antiferromagnetic phase transition.

A non-reciprocal X-ray magnetic linear dichroism spectrum was recorded at beamline ID12 with a Cr doped crystal $(V_{1-x}Cr_x)_2O_3$ [27]. According to neutron diffraction data [49], the space–time group of the AFM monoclinic low temperature phase below T_N should be mostly 2 due to a transfer of magnetic moments onto oxygen atoms. If this interpretation is correct, then the low temperature monoclinic phase of V_2O_3 *should* be magnetoelectric. We have to admit that we are not aware of any successful measurements of the magnetoelectric susceptibility in V_2O_3. The reason for the failure of the first experiment reported by Astrov [50] is apparently related to the fact that the first order phase transition from the corundum to the monoclinic phase in pure V_2O_3 is crystal-destructive. This is why we tried to detect a non-reciprocal XLD signal with a Cr-doped $(V_{1-x}Cr_x)_2O_3$ single crystal for which $x = 0.028$. At this concentration not only T_N raises from 150 K to ca. 181 K, but also the electric resistivity is substantially increased in the paramagnetic phase. Here, we used the same crystal as for previous resonant X-ray scattering experiments carried out at the ESRF beamline ID20 [51]: this Cr-doped crystal($1.0 \times 0.8 \times 0.05$ mm^3) was initially assumed to have been cleaved perpendicularly to the hexagonal **c** axis, but it was realized later that it was slightly miscut. Neutron diffraction experiments suggested that, in the low temperature (monoclinic) phase, the magnetic moments ($1.2\mu_B$ per V atom) would be rotated by ca. 71° with respect to the hexagonal **c** axis: the system could then perfectly exhibit a non-reciprocal XMLD.

As illustrated in Fig. 6, we measured a quite significant nr-XMLD signal at the vanadium K-edge (ca. 1% of the edge jump) after magnetoelectric annealing. For the sake of comparison, the deconvoluted V K-edge XANES spectrum is also shown. The non-reciprocal XMLD spectra reproduced in Fig. 6 were recorded after a magnetoelectric annealing process conducted in the geometry $\mathbf{E}\|\mathbf{H}\|\mathbf{k}$ with **c** tilted away from **k** by approximately 10°. Because the signal was found to change its sign when the annealing was performed with parallel or antiparallel electric and magnetic fields and to vanish above the Néel temperature $T_N = 181$ K, we feel that there is very little doubt left regarding the non-reciprocal character of this signal. The orientations of the crystallographic axes **a** and **b** were unfortunately unknown in this experiment: this makes it impossible to clarify whether the non-reciprocal dichroism that was measured is to be interpreted as a Jones cross-XMLD or as a true non-reciprocal XMLD. This dichroism can be most easily understood if the inversion symmetry is broken by the magnetic order as expected in the space–time magnetoelectric group 2: our result would basically support the early interpretation proposed by Word and his colleagues [49]. If this is true, and if the magnetoelectric annealing procedure can be kept fully under control, then non-reciprocal X-ray magnetic linear dichroism could develop as a powerful technique to unravel hidden space–time symmetry in magnetoelectric systems.

Let us mention here that the existence of nr-XMLD effect was confirmed recently by Kubota et al. [52]. These authors have measured nr-XMLD spectra at the Fe K-edge in a polar ferrimagnetic crystal of $GaFeO_3$. They called this effect *X-ray non-reciprocal Directional Dichroism* (XNDD) to emphasize the fact that its sign depends on whether the X-ray propagation direction is parallel or antiparallel to the outer product of the magnetization and electric-polarization vectors in the sample. The experiment reported by Kubota et al. [52] benefited from the tremendous advantage that no magnetoelectric annealing was needed because the crystal can be more easily ordered as a weak ferromagnet.

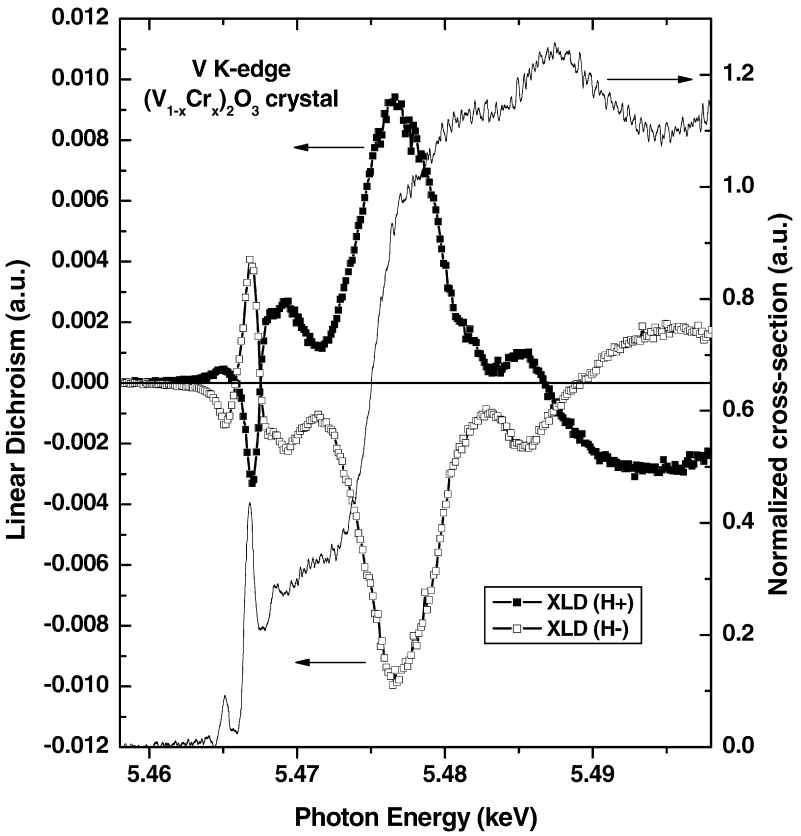

Fig. 6. Non-reciprocal XLD spectra recorded at the V K-edge in the monoclinic AFI phase of the $(V_{1-x}Cr_x)_2O_3$ crystal. The magneto-electric annealing was performed either with parallel (+) or antiparallel (–) electric and magnetic fields. Deconvoluted V K-edge XANES spectrum is also shown for comparison.

5.2. X-ray Magnetochiral Dichroism (XMχD)

Let us introduce below another non-reciprocal effect which we called *X-ray Magnetochiral Dichroism* (XMχD) because it exhibits a marked analogy with a long expected optical effect [53,54] that was finally observed in 1997 by Rikken [55] using visible light. Strangely enough, this new type of X-ray dichroism refers to differences in the absorption cross-section measured with an *unpolarized* X-ray beam when the sign of the magnetization is inverted in a so-called magnetochiral medium. In such systems, both inversion and time-reversal symmetries are again broken so that these crystals are expected to be once again magnetoelectric. However, only 31 magnetoelectric groups [56] out of 58 are compatible with the observation of a magnetochiral effect. Those groups have all in common the characteristic property that their rank-2 ME tensor should have *antisymmetric* off-diagonal terms.

The first XMχD spectrum was measured using a single crystal of chromium sesquioxyde (Cr_2O_3) cooled down to its antiferromagnetic phase. Recall that Cr_2O_3 is the generic example of magnetoelectric solids with a convenient transition temperature at 307 K. For the same reasons as explained in the previous sub-section, single domains had again to be grown by magnetoelectric annealing with either parallel or antiparallel electric and magnetic fields. The XMχD spectra were recorded at the Cr K-edge in the fluorescence excitation mode. We produced artificially an unpolarized light by incoherent superposition of fluorescence excitation spectra recorded with right and left circularly polarized incident photons: $F_0 = F_{rcp} + F_{lcp}$. The Cr K-edge XMχD spectra displayed in Fig. 7 were measured at 50 K by calculating the difference between unpolarized XANES spectra recorded for two 180° domains grown via magnetoelectric annealing with external electric and magnetic fields either parallel or antiparallel to each other. The deconvoluted unpolarized XANES spectrum recorded with an equidomain crystal with **k** parallel to the **c** axis of the crystal is also shown for the sake of comparison. Since rotational isotropy of space is broken when single domains

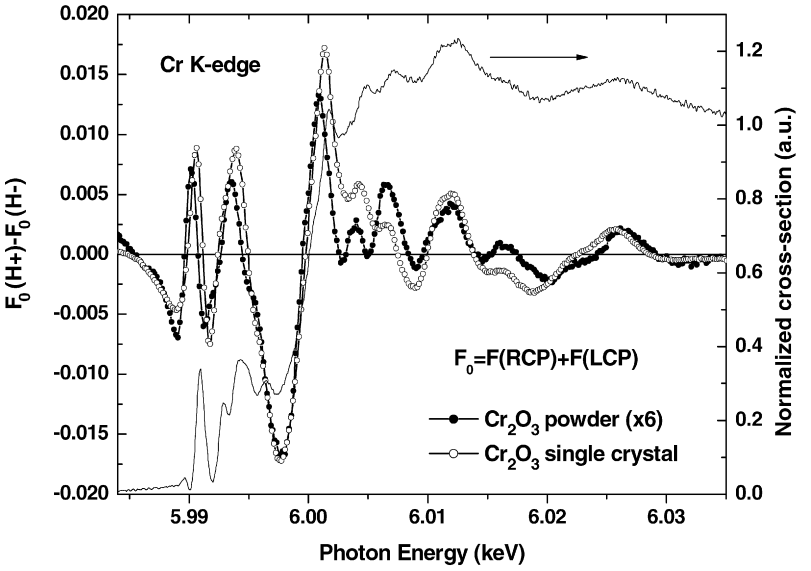

Fig. 7. Cr K-edge XMχD spectra of a (001) single crystal and a powdered pellet of Cr_2O_3 for $\mathbf{k}\|\mathbf{c}\|t\mathbf{E}\|\mathbf{H}$. The signal from the powder is multiplied by 6. XMχD spectra refer to the difference of isotropic spectra measured on two opposite domains grown by magnetoelectric annealing. For the sake of comparison, deconvoluted XANES spectrum is shown.

are grown by magnetoelectric annealing along the direction of (**E**, **H**), one may anticipate that XMχD spectra could be recorded as well with powdered samples. This was confirmed experimentally: using a pellet of Cr_2O_3 powder, we were able to record XMχD spectra that look very similar to the previous ones except that the intensity of the dichroism was reduced by a factor of 6.

Surprisingly enough, the magnetic group $\bar{3}'m'$ of Cr_2O_3 did not belong to the 31 groups that are compatible with the existence of the magnetochiral effect. To explain our experimental data correctly then the true magnetic group of Cr_2O_3 cannot be $\bar{3}'m'$ (as deduced from neutron data); the symmetry of the group must be lower. There may be several ways to explain such a reduction of magnetic symmetry. As far as we are concerned, there is no doubt that the spin configuration at the chromium sites deduced from neutron data should be quite correct, but it is our interpretation that there might be some magnetic polarization of the oxygen atoms affecting the *orbital* magnetism. It was precisely pointed out by Shirane et al. [57] more than 30 years ago, that the covalent character in the Cr–O bonds involved a small spin transfer from the chromium $3d$-orbitals to the oxygen $2p$ shell, but these authors noted that such a transferred moment was *too small* to be detected in neutron diffraction experiments. Recall that an asymmetric twist of the oxygen planes is already responsible for a reduction of the local symmetry of the Cr atoms from C_{3v} to C_3 [58]. As pointed out in [59], the angular momentum unquenched by covalent bonding, with a different quantization axis than the spins, could be a widespread phenomenon in antiferromagnetic solids. It is precisely our interpretation that the orbital contribution to the magnetoelectric tensor (which was systematically neglected so far) could now be measured with XMχD and could perfectly be responsible for a lower symmetry. If this is true, then one should seek for a magnetoelectric group consistent with both X-ray optical activity and the well-established magnetoelectric susceptibility measurements in antiferromagnetic crystals: the only magnetic group that could reconcile all published studies regarding the magnetic properties of Cr_2O_3 is $\bar{3}'$. We, therefore, propose this group as the true magnetic group describing the spin *and* orbital magnetoelectric effects in Cr_2O_3 [26].

6. Effective operators of X-ray Optical Activity

It is now well recognized that much of the success of X-ray Magnetic Circular Dichroism is to be credited to the availability of the magneto-optical sum rules [60,61]. These sum rules made it possible to establish a direct link between the integrated XMCD spectra and the expectation value of the z component of several magnetic operators: $\langle \mathbf{L_z} \rangle$, $\langle \mathbf{S_z} \rangle$ and $\langle \mathbf{T_z} \rangle$. A similar approach was first proposed by Natoli [21] for XNCD, but no clear physical meaning of the effective operator responsible for XNCD could be given. Using the powerful method of group generators, Carra

and his collaborators derived a whole set of sum rules related to X-ray optical activity [62–65]. A key achievement was to show that all effective operators responsible for X-ray detected OA could be built from a triad of mutually orthogonal vector operators:

- $\mathbf{n} = \mathbf{r}/\ r$ which is a time-reversal *even*, polar vector associated with the electric dipole moment;
- the orbital angular momentum $\mathbf{L}$ which is a time-reversal *odd* axial vector; and
- the toroidal vector $\boldsymbol{\Omega} = [(\mathbf{n} \times \mathbf{L}) - (\mathbf{L} \times \mathbf{n})]/2$ which is odd with respect to both parity and time-reversal.

Here, $\boldsymbol{\Omega}$ was rapidly identified with the orbital *anapole* moment as defined in textbooks [66]. Recall that the concept of anapole was first introduced in 1958 by Zel'dovich [67] from symmetry considerations, but essentially as a useful tool to describe parity-violating interactions. Up to five spherical operators are required for a full description of the effects related to X-ray detected OA:

- The ground state expectation value of the z component of the orbital anapole moment $\langle \boldsymbol{\Omega}_\mathbf{z} \rangle$ was shown to be the key effective operator for XMχD;
- The effective operator responsible for XNCD should be the time-reversal *even*, rank-2 pseudo-deviator associated with the tensor product: $[\mathbf{L} \otimes \boldsymbol{\Omega}]^{(2)}$;
- Regarding the vector part of OA, the effective operator should be a polar vector ($\mathbf{L^2} \cdot \mathbf{n}$), which, as pointed out by Marri and Carra [65], may be responsible for ferroelectric order;
- The time-reversal odd rank-2 pseudo-deviator defined as $[\mathbf{L} \otimes \mathbf{n}]^{(2)}$ is an effective operator that should contribute primarily to non-reciprocal XMLD;
- The last effective operator to be considered is an orbital septor $[[\mathbf{L} \otimes \mathbf{L}]^{(2)} \otimes \boldsymbol{\Omega}]^{(3)}$. It may contribute to second order terms in the sum rules derived for XMχD and non-reciprocal XMLD.

The physical implications of the sum rules as well as the practical conditions of their application were discussed elsewhere [11]. The case of Cr_2O_3 looks particularly interesting. In a controversial paper, Di Matteo and Natoli [68] claimed that the largest contribution should come from the septor terms. This is, however, contradicted by our experiment carried on the powdered sample and illustrated with Fig. 7. One may easily establish [11] that the XMχD signal in powdered samples should be reduced by the factor ≈ 5.5 if the effective operator was $\boldsymbol{\Omega}$, whereas it should become hardly measurable ($\leqslant 0.05$) if the effective operator was the septor. Our measurements nicely confirm the first option. On the other hand, the XMχD sum rule offers a unique possibility to estimate the expectation value of the orbital anapole moment in Cr_2O_3: $\langle \boldsymbol{\Omega}_z \rangle \approx 0.03$ a.u. The corresponding value of the orbital anapole is indeed fairly small in comparison to the recent estimates given for spin anapoles [11]. Our result looks therefore fully consistent with the early remark we made that it would be very difficult – if not simply impossible – to access the orbital part of the magnetoelectric tensor using conventional magnetoelectric susceptibility measurements.

There is another interesting remark that could be drawn from the XNCD sum rule: it clearly appears that the effective operator associated with natural X-ray detected OA is the time-reversal *even* direct product of two time-reversal *odd* operators that are both related to orbital magnetism. This result establishes a direct link between OA and magnetism. Let us recall here that Pasteur [69] tried hard for many years to show that chirality and magnetism were connected but he could not prove it within the knowledge of his time.

7. Conclusion

It was the aim of this paper to try to convince the reader that X-ray detected OA could develop as a new, *element and orbital selective* spectroscopy that could be a unique tool to study orbital magnetism in parity non-conserving solids. The sum rules give us access to the ground state expectation values of orbital operators. Applied to non-reciprocal X-ray detected OA spectra these sum rules might reveal hidden space–time symmetry properties in magnetoelectric crystals when the angular momentum, which is partially unquenched, has a quantization axis different to that of the spins.

Acknowledgements

The authors wish to acknowledge a long standing and very fruitful collaboration with Christian Brouder and Paolo Carra. The authors are particularly indebted to Efim Katz for many stimulating discussions over the past years. Acknowledgments are also due to Yves Petroff for his valuable comments and permanent encouragement.

References

[1] D.F.M. Arago, Mémoires de l'Institut de France 12 (1811) 93.
[2] J.-B. Biot, Mémoires de l'Institut de France 13 (1812) 218.
[3] M. Faraday, Philos. Trans. 3 (1846) 1.
[4] L.D. Landau, E.M. Lifshitz, Electrodynamics of Continuous Media, Pergamon Press, New York, 1960.
[5] J. Goulon, C. Goulon-Ginet, A. Rogalev, V. Gotte, C. Malgrange, C. Brouder, C.R. Natoli, J. Chem. Phys. 108 (1998) 6394.
[6] L. Alagna, T. Prosperi, S. Turchini, J. Goulon, A. Rogalev, C. Goulon-Ginet, C.R. Natoli, R.D. Peacock, B. Stewart, Phys. Rev. Lett. 80 (1998) 4799.
[7] J. Goulon, C. Goulon-Ginet, A. Rogalev, G. Benayoun, C. Brouder, C.R. Natoli, J. Synchroton Radiat. 6 (1999) 673.
[8] B. Stewart, R.D. Peacock, L. Alagna, T. Prosperi, S. Turchini, J. Goulon, A. Rogalev, C. Goulon-Ginet, J. Am. Chem. Soc. 121 (1999) 10233.
[9] J. Goulon, in: E. Beaurepaire, B. Carriére, J.P. Kappler (Eds.), Rayonnement Synchrotron Polarisé, Electrons Polarisés et Magnétisme, IPCMS, Strasbourg, 1990, p. 333.
[10] J. Goulon, A. Rogalev, F. Wilhelm, N. Jaouen, C. Goulon-Ginet, C. Brouder, J. Phys.: Condens. Matter 15 (2003) S633.
[11] J. Goulon, A. Rogalev, F. Wilhelm, C. Goulon-Ginet, P. Carra, I. Marri, Ch. Brouder, J. Exp. Theor. Phys. 97 (2003) 402.
[12] A.D. Buckingham, Adv. Chem. Phys. 12 (1968) 107.
[13] L.D. Barron, Molecular Light Scattering and Optical Activity, Cambridge University Press, Cambridge, 1982.
[14] J. Goulon, C. Goulon-Ginet, A. Rogalev, V. Gotte, C. Brouder, C. Malgrange, Eur. Phys. J. B 12 (1999) 373.
[15] Ch. Brouder, J. Phys.: Condens. Matter 2 (1990) 701.
[16] H.A. Lorentz, Proc. Acad. Amsterdam 24 (1921) 333.
[17] J. Pastrnak, K. Vedam, Phys. Rev. B 3 (1971) 2567.
[18] G. Dräger, R. Frahm, G. Materlick, O. Brümmer, Phys. Status Solidi B 146 (1988) 287.
[19] D. Cabaret, C. Brouder, M.-A. Arrio, Ph. Sainctavit, Y. Joly, A. Rogalev, J. Goulon, J. Synchrotron Radiat. 8 (2001) 460.
[20] J. Jerphagnon, D.S. Chemla, J. Chem. Phys. 65 (1976) 1522.
[21] C.R. Natoli, Ch. Brouder, Ph. Sainctavit, J. Goulon, C. Goulon-Ginet, A. Rogalev, Eur. Phys. J. B 4 (1998) 1.
[22] M. Okutani, T. Jo, P. Carra, J. Phys. Soc. Jpn 68 (1999) 3191.
[23] Ch. Brouder, C.R. Natoli, Ph. Sainctavit, J. Goulon, C. Goulon-Ginet, A. Rogalev, J. Synchrotron Radiat. 6 (1999) 261.
[24] I.E. Dzyaloshinskii, Sov. Phys. JETP 10 (1960) 628.
[25] A.J. Freeman, H. Scmhid (Eds.), Magnetoelectric Interaction Phenomena in Crystals, Gordon & Breach, London, 1975.
[26] J. Goulon, A. Rogalev, F. Wilhelm, C. Goulon-Ginet, P. Carra, D. Cabaret, Ch. Brouder, Phys. Rev. Lett. 88 (2002) 237401.
[27] J. Goulon, A. Rogalev, C. Goulon-Ginet, G. Benayoun, L. Paolasini, Ch. Brouder, C. Malgrange, P.A. Metcalf, Phys. Rev. Lett. 85 (2000) 4385.
[28] J. Goulon, N. Jaouen, A. Rogalev, F. Wilhelm, C. Goulon-Ginet, Ch. Brouder, Y. Joly, E.N. Ovchinnikova, V.E. Dmitrienko, J. Phys.: Condens. Matter 19 (2007) 156201.
[29] J. Goulon, A. Rogalev, C. Gauthier, C. Goulon-Ginet, S. Pasté, R. Signorato, C. Neuman, L. Varga, C. Malgrange, J. Synchrotron Radiat. 5 (1998) 232.
[30] A. Rogalev, J. Goulon, C. Goulon-Ginet, C. Malgrange, in: E. Beaurepaire, et al. (Eds.), Magnetism and Synchrotron Radiation, in: Lecture Notes in Physics, vol. 565, Springer, Berlin, 2001, p. 60.
[31] P. Elleaume, J. Synchrotron Radiat. 1 (1994) 19.
[32] A. Rogalev, J. Goulon, G. Benayoun, P. Elleaume, J. Chavanne, C. Penel, P. Van Vaerenbergh, Proc. SPIE 3773 (1999) 275.
[33] J. Goulon, C. Goulon-Ginet, A. Rogalev, V. Gotte, Ch. Brouder, C. Malgrange, Eur. Phys. J. B 12 (1999) 373.
[34] J. Goulon, C. Goulon-Ginet, A. Rogalev, G. Benayoun, Ch. Brouder, C.R. Natoli, J. Synchrotron Radiat. 7 (2000) 182.
[35] C. Malgrange, L. Varga, C. Giles, A. Rogalev, J. Goulon, Proc. SPIE 3773 (1999) 326.
[36] J. Kaniauskas, Liet. Fiz. Rink. XIV (1974) 463 (in Russian).
[37] W. Voigt, Ann. Phys. (Leipzig) 18 (1905) 651.
[38] F.I. Fedorov, Opt. Spectrosc. (USSR) 6 (1959) 237.
[39] F.I. Fedorov, B.V. Bokut, A.F. Konstantinova, Sov. Phys. Crystallogr. 7 (1963) 738.
[40] E.L. Ivchenko, S.A. Permogorov, A.V. Sel'kin, JETP Lett. 27 (1978) 24.
[41] E.B. Graham, R.E. Raab, Proc. R. Soc. A (London) 430 (1990) 593.
[42] N. Jaouen, F. Wilhelm, A. Rogalev, J. Goulon, J.M. Tonnerre, AIP Conf. Proc. 705 (2004) 1134.
[43] G. Van der Laan, B.T. Thole, G.A. Sawatzky, J.B. Goedkoop, J.C. Fuggle, J.M. Esteva, R. Karnatak, J.P. Remeika, H.A. Dabkowska, Phys. Rev. B 34 (1986) 6529.
[44] R.R. Birss, R.G. Shrubsall, Philos. Mag. 15 (1967) 687.
[45] R.M. Hornreich, S. Shtrikman, Phys. Rev. 171 (1968) 1065.
[46] E.B. Graham, R.E. Raab, Philos. Mag. 66 (1992) 269.

[47] V.A. Markelov, M.A. Novikov, A.A. Turkin, JETP Lett. 25 (1977) 378.
[48] B.B. Krichevtsov, V.V. Pavlov, R.V. Pisarev, V.N. Gridnev, J. Phys.: Condens. Matter 5 (1993) 8233.
[49] R.E. Word, S.A. Werner, W.B. Yelon, J.M. Honig, S. Shivashankar, Phys. Rev. B 23 (1981) 3533.
[50] B.I. Al'shin, D.N. Astrov, Sov. Phys. JETP 17 (1963) 809.
[51] L. Paolasini, C. Vettier, F. de Bergevin, F. Yakhou, D. Mannix, A. Stunault, W. Neubeck, M. Altarelli, M. Fabrizio, P.A. Metcalf, J.M. Honig, Phys. Rev. Lett. 82 (1999) 4719.
[52] M. Kubota, T. Arima, Y. Kaneko, J.P. He, X.Z. Yu, Y. Tokura, Phys. Rev. Lett. 92 (2004) 137401.
[53] N.B. Baranova, B.Ya. Zel'dovich, Mol. Phys. 38 (1979) 1085.
[54] L.D. Barron, J. Vrbancich, Mol. Phys. 51 (1984) 715.
[55] G.L.J.A. Rikken, E. Raupach, Nature 390 (1997) 493.
[56] V.M. Dubovik, Sov. Phys. Crystallogr. 32 (1988) 314.
[57] E.J. Samuelsen, M.T. Hutchings, G. Shirane, Physica 48 (1970) 13.
[58] M. Vallade, Ph.D. Thesis, Université J. Fourier, Grenoble, 1968 (Chapter IV).
[59] V.P. Plakthy, Solid State Commun. 79 (1991) 313.
[60] B.T. Thole, P. Carra, F. Sette, G. van der Laan, Phys. Rev. Lett. 68 (1992) 1943.
[61] P. Carra, B.T. Thole, M. Altarelli, X. Wang, Phys. Rev. Lett. 70 (1993) 694.
[62] P. Carra, R. Benoist, Phys. Rev. B 62 (2000) R7703.
[63] P. Carra, J. Magn. Magn. Mat. 233 (2001) 8.
[64] P. Carra, A. Jerez, I. Marri, Phys. Rev. B 67 (2003) 045111.
[65] I. Marri, P. Carra, Phys. Rev. B 69 (2004) 113101.
[66] I.B. Khriplovich, Parity Non-Conservation in Atomic Phenomena, Gordon and Breach, New York, 1991.
[67] Ya.B. Zel´dovich, Sov. Phys. JETP 6 (1958) 1184.
[68] S. Di Matteo, C.R. Natoli, Phys. Rev. B 66 (2002) 212413.
[69] L. Pasteur, Rev. Sci. 7 (1884) 2.